Experimental Neurology 236 (2012) 151–160

Contents lists available at SciVerse ScienceDirect

Experimental Neurology

journal homepage: www.elsevier.com/locate/yexnr

Retinal changes in an experimental model of early type 2 diabetes in rats characterized by non-fasting hyperglycemia

Ezequiel M. Salido [a], Nuria de Zavalía [a], Laura Schreier [b], Andrea De Laurentiis [c], Valeria Rettori [c], Mónica Chianelli [a], María Inés Keller Sarmiento [a], Pablo Arias [d,1], Ruth E. Rosenstein [a,*,1]

[a] Laboratory of Retinal Neurochemistry and Experimental Ophthalmology, Department of Human Biochemistry, School of Medicine, University of Buenos Aires/CEFyBO, CONICET, Buenos Aires, Argentina
[b] Laboratory of Lipids and Lipoproteins, Department of Clinical Biochemistry, School of Pharmacy and Biochemistry-INFIBIOC, University of Buenos Aires, Buenos Aires, Argentina
[c] CEFyBO, CONICET, Buenos Aires, Argentina
[d] Physiology Department, School of Medical Sciences, Universidad Nacional de Rosario, Santa Fe, Argentina

ARTICLE INFO

Article history:
Received 6 March 2012
Revised 11 April 2012
Accepted 12 April 2012
Available online 21 April 2012

Keywords:
Type 2 diabetes mellitus
Experimental model
Diabetic retinopathy
Electroretinogram

ABSTRACT

Diabetic retinopathy is a leading cause of acquired blindness in young, but also in elder adults, mostly affected by type 2 diabetes mellitus (T2DM). The aim of this work was to develop an experimental model of early human T2DM in adult rats, and to analyze retinal functional, morphological, and biochemical changes arising during the early stages of the moderate metabolic derangement. For this purpose, animals were divided in four groups: adult male *Wistar* rats receiving: tap water and citrate buffer i.p. (group 1), tap water with 30% sucrose and citrate buffer i.p. (group 2), tap water and 25 mg/kg i.p streptozotocin (STZ, group 3), or 30% sucrose and STZ (group 4). Fasting and postprandial glycemia, fructosamine and serum insulin levels were assessed. In addition, i.p. glucose and insulin tolerance tests were performed. Retinal function (electroretinogram, ERG) and morphology (optical microscopy), retinal nitric oxide synthase (NOS) activity (using ^{3}H-arginine), lipid peroxidation (thiobarbituric acid reactive substances, TBARS), and TNFα levels (ELISA) were evaluated. At 6 and 12 weeks of treatment, animals which received a sucrose-enriched diet and STZ showed significant differences in most metabolic tests, as compared with the other groups. At 12 weeks of treatment, a significant decrease in the ERG a- and b- wave and oscillatory potential amplitudes, and a significant increase in retinal NOS activity, TBARS, TNFα, glial fibrillary acidic protein in Müller cells, and vascular endothelial growth factor levels were observed. These results indicate that the combination of diet-induced insulin resistance and a slight secretory impairment resulting from a low-dose STZ treatment mimics some features of human T2DM at its initial stages, and provokes significant retinal alterations.

Introduction

About 350 million people across the globe are estimated to have diabetes (Danaei et al., 2011), and type 2 diabetes mellitus (T2DM) accounts for roughly 90% of all diagnosed cases (American Diabetes Association, 2008). Diabetic retinopathy (DR), one of the most feared complications of diabetes, is a leading cause of acquired blindness in young, as well as elder adults, mostly affected by T2DM (King et al., 1998; The Eye Diseases Research Prevalence Research Group-National Eye Institute, 2004). Experimental, epidemiological, and large scale intervention studies, such as the Diabetes Control and Complications Trial, and the UK Prospective Diabetes Study Group have demonstrated that hyperglycemia is a major trigger for its development, and lowering of blood glucose levels is essential for preventing or arresting DR development (Diabetes Control and Complications Trial Research Group, 1993; UK Prospective Diabetes Study (UKPDS) Group, 1998). In inadequately controlled patients with diabetes mellitus, the retinal microvasculature is constantly exposed to high glucose levels, and this insult results in many structural and functional alterations (UK Prospective Diabetes Study (UKPDS) Group, 1998). Current treatments for DR such as laser photocoagulation, corticosteroids,

Abbreviations: AUC, area under the curve; DR, diabetic retinopathy; ERG, electroretinogram; GCL, ganglion cell layer; GFAP, glial fibrillary acidic protein; HbA1c, glycosylated hemoglobin; IPGTT, intraperitoneal glucose tolerance; IPITT, intraperitoneal insulin tolerance test; MDA, malondialdehyde bis-dimethyl acetal; NOS, nitric oxide synthase; OP, oscillatory potential; SDT, spontaneously diabetic Torii; STZ, streptozotocin; TBARS, thiobarbituric acid reactive substances; T2DM, type 2 diabetes mellitus; TNF-α, tumor necrosis factor α; VEGF, vascular endothelial growth factor.

* Corresponding author at: Departamento de Bioquímica Humana, Facultad de Medicina, CEFyBO, Paraguay 2155, 5°P, (1121), Universidad de Buenos Aires, CONICET, Buenos Aires, Argentina. Fax: +54 11 4508 3672x31.
E-mail address: ruthr@fmed.uba.ar (R.E. Rosenstein).
[1] Both authors contributed equally to this work.

0014-4886/$ – see front matter © 2012 Elsevier Inc. All rights reserved.
doi:10.1016/j.expneurol.2012.04.010

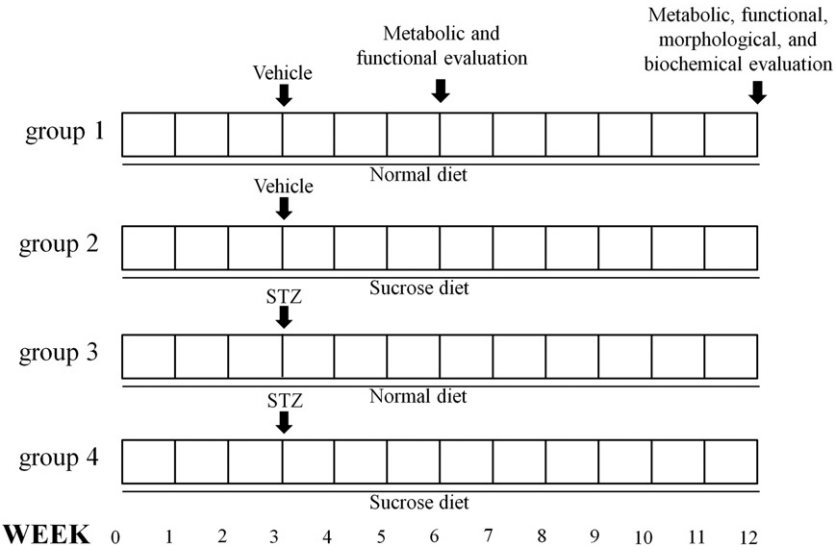

Fig. 1. Experimental groups. Animals were submitted to a normal diet (groups 1 and 3) or a sucrose enriched diet (groups 2 and 4) for 12 weeks. At the third week, animals were i.p. injected with vehicle (groups 1 and 2) or SZT (groups 3 and 4). Metabolic and retinal studies were performed at 6 and 12 weeks of treatment.

or anti-vascular endothelial growth factor agents are indicated for advanced DR, but have significant adverse effects. Therefore, new therapeutic treatments for the early stages of DR are needed. Understanding the molecular mechanisms of retinal damage associated with T2DM should help identify therapies to treat/postpone this sight-threatening complication of diabetes. For this purpose, a large number of genetically modified animal models including transgenic, generalized knockout, and tissue specific knockout mice have been employed. However, a typical diabetic profile is not always seen in these genetically induced models, nor do they absolutely mimic the pathogenesis of human T2DM (Matsumura et al., 2005; Movassat et al., 1995) since these gene mutations are extremely rare in human populations. Similarly, animal models of T2DM induced by removal of a portion of the pancreas (Portha et al., 1989) are not representative of the T2DM etiology in humans, which is typically preceded by obesity (Bray, 2004; Goralski and Sinal, 2007). In order to better understand the events which precede and precipitate the onset of T2DM, some nutritional animal models have been also developed (Mühlhausler, 2009; Shafrir et al., 2006; Srinivasan and Ramarao, 2007; Surwit et al., 1988).

Initially, the natural history of T2DM includes a period of normal or near-normal fasting plasma glucose levels and marked postprandial glycemic excursions (Monnier et al., 2007). However, the impact of these hyperglycemic spikes on retinal function is still unknown. Comprehension of the abnormalities that characterize the initial phases of DR may reveal therapeutic targets that could effectively block the progression of the disease. To our knowledge, there are no animal models that allow for the study of early retinal complications associated to mild fasting hyperglycemia and postprandial glycemic spikes. Thus, the present study was conceived in order to: a) develop an experimental model more closely mimicking the natural history of human T2DM, inducing insulin resistance in adult rats by means of a sucrose-rich diet, and then reducing pancreatic insulin release using low doses of streptozotocin (STZ), and b) analyze metabolic changes and functional, morphological, and biochemical alterations arising in the retina during the early stages of the moderate metabolic derangement.

Materials and methods

Animals

Male *Wistar* rats (400 ± 50 g) were housed in a standard animal room with food and water *ad libitum* under controlled conditions of humidity, temperature (21 ± 2 °C), and luminosity (200 lux), under a 12-hour light /12-hour dark lighting schedule (lights on at 7:00 AM). All animal procedures were in strict accordance with the ARVO Statement for the Use of Animals in Ophthalmic and Vision Research. The ethics committee of the University of Buenos Aires School of Medicine, (Institutional Committee for the Care and Use of Laboratory Animals, (CICUAL)) approved this study.

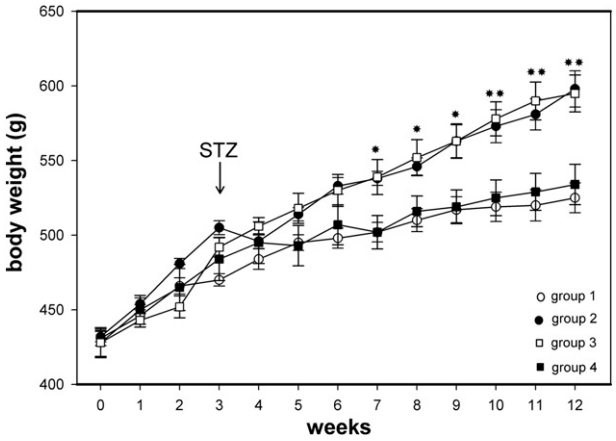

Fig. 2. Temporal course of body weight for all the experimental groups. Body weight significantly increased throughout the experiment in all groups, but from week 7 to 12, it was significantly higher in groups receiving sucrose (groups 2 and 4) than in those which did not (groups 1 and 3). Data are mean ± SEM ($n = 10$ animals/group). $^{*}p<0.05$, $^{**}p<0.01$ for groups 2 and 4 vs. group 1 and group 3, by Tukey's test.

Feeding and treatments

Four groups of rats were included in the present study, as depicted in Fig. 1: control animals receiving a standard commercial rat chow and tap water (group 1, control); animals receiving a standard commercial rat chow and 30% sucrose in the drinking water (group 2, sucrose); animals receiving a standard commercial rat chow and tap water, which were intraperitoneally (i.p.) injected with streptozotocin (STZ, 25 mg/kg) (group 3, STZ); animals receiving a standard commercial rat chow and 30% sucrose in the drinking water, which were i.p. injected with STZ (25 mg/kg) three weeks after receiving 30% sucrose in the drinking water (group 4, sucrose + STZ). Animals from groups 1 and 2 were injected with vehicle (citrate buffer) at the same time at which group 3 and 4 were injected with STZ. Sucrose solution was replaced every two days. Animals were weighed weekly up to 12 weeks of treatment.

Blood glucose measurements

Plasma glucose levels were determined in tail vein blood samples using the Accu-Check Performa blood glucose meter (Roche Diagnostic, Mannheim, Germany). In some experiments, animals were fasted for 4 h before the measurements, whereas in other experiments, plasma glucose levels were assessed at 11.00 or 23.00 h in non fasted animals.

Intraperitoneal glucose tolerance (IPGTT) and intraperitoneal insulin tolerance test (IPITT)

IPGTT and IPITT were performed at weeks 6 and 12. Animals were restricted of food and water 4 h before the experiments. For the IPGTT, rats received an i.p. injection of glucose (1 g/kg body weight). Blood samples for plasma glucose measurement were collected from the tail vein at time 0 (before glucose injection) and 30, 60, 90 and 120 min after glucose administration. The area under the curve (AUC) was calculated using the trapezoidal rule estimation.

For the IPITT, rats were intraperitoneally injected with regular human insulin (0.75 IU/kg body weight). Again, blood samples were taken from the tail vein at time 0 (before insulin injection) and 15, 30, 45 and 60 minutes after insulin administration. Insulin sensitivity was estimated from the slope of the 0–60 min glucose disappearance rate. This slope was determined by linear regression as previously described (Srinivasan et al., 2005).

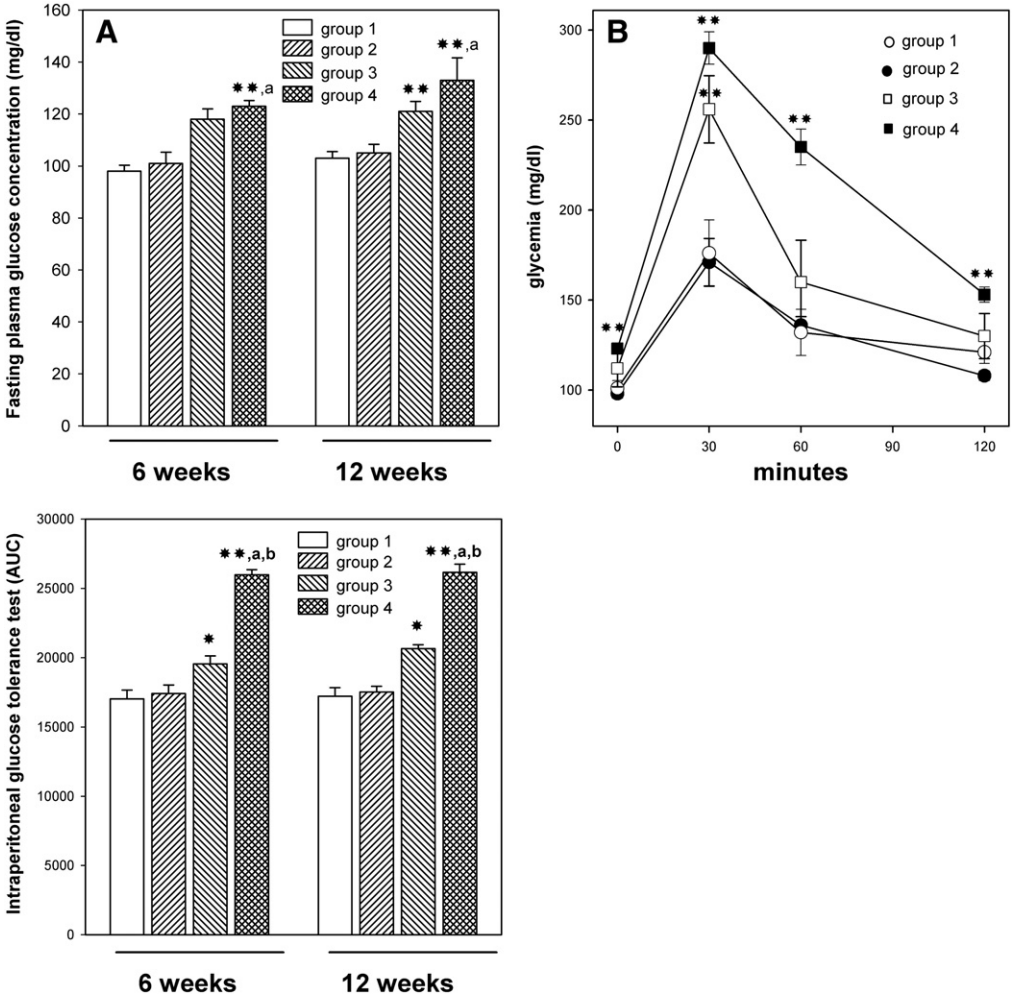

Fig. 3. Glucose metabolism assessed at 6 and 12 weeks of treatment. Panel A: At 6 and 12 weeks of treatment, fasting plasma glucose levels were significantly higher in group 4 than in groups 1 and 2, whereas at 12 weeks of treatment, this parameter was significantly higher in group 3 than in group 1. Panel B: Mean plasma glucose concentrations in response to an intraperitoneal glucose challenge assessed before and 30, 60 and 120 min after 1 g/kg glucose injection. Panel C: AUC of the IPGTT. At both time points, higher values of the AUC were observed in group 4 than in groups 1, 2, and 3, while group 3 only differed from group 1. Data are the mean ± SEM ($n = 10$ animals per group); $^{*}p<0.05$, $^{**}p<0.01$ vs. group 1, a: $p<0.01$ vs. group 2, b: $p<0.01$ vs. group 3, by Tukey's test.

Fructosamine and insulin level assessment

Rats were fasted for 4 h. Blood was collected from the tail vein; plasma was separated by centrifugation at 3500 ×*g* for 15 minutes and frozen at −80 °C. Serum fructosamine concentrations were determined using a commercial test kit (Fructosamina AA, Wiener, Rosario, Argentina), used in accordance with the manufacturer´s instructions. Plasma insulin levels were determined using a specific immunoassay kit (Rat Insulin ELISA Kit EZRMI-13K, Linco Research, St. Charles, Missouri, USA).

Electroretinography

Electroretinographic activity was assessed at 6 and 12 weeks of treatment, as previously described (Moreno et al., 2005). Briefly, after 6 h of dark adaptation, rats were anesthetized under dim red illumination, pupils were dilated, and the cornea was intermittently irrigated with balanced salt solution to maintain the baseline recording and to prevent keratopathy. Rats were placed facing the stimulus at a distance of 20 cm. A reference electrode was placed through the ear, a grounding electrode was attached to the tail, and a gold electrode was placed in contact with the central cornea. A dim red light was used to enable accurate electrode placement. ERGs were recorded from both eyes simultaneously and ten responses to flashes of unattenuated white light (5 ms, 0.2 Hz) from a photic stimulator (light-emitting diodes) set at maximum brightness were amplified, filtered (1.5-Hz low-pass filter, 1000 high-pass filter, notch activated) and averaged (Akonic BIO-PC, Argentina). The a-wave was measured as the difference in amplitude between the recording at onset and trough of the negative deflection, and the b-wave amplitude was measured from the trough of the a-wave to the peak of the b-wave. Runs were repeated 3 times with 5 min-intervals to confirm consistency. Mean values from each eye were averaged, and the resultant mean value was used to compute the group means a- and b-wave amplitude ± SEM. The mean peak-to-peak amplitudes of the responses from each group were compared.

Oscillatory potentials (OPs) were assessed as previously described (Moreno et al., 2005). Briefly, the same photic stimulator with a 0.2 Hz frequency and filters of high (300 Hz) or low (100 Hz) frequency were used. The OP amplitude was estimated by measuring the heights from the baseline drawn between the troughs of successive wavelets to their peaks. The sum of three OPs was used for statistical analysis.

Histological examination

Rats were killed and their eyes were immediately enucleated, immersed for 24 h in 4% formaldehyde in 0.1 M phosphate buffer (pH 7.2), and embedded in paraffin. Eyes were sectioned (5 μm) along the vertical meridian through the optic nerve head. Microscopic images were digitally captured with a Nikon Eclipse E400 microscope (illumination: 6-V halogen lamp, 20 W, equipped with a stabilized light source) via a Nikon Coolpix s10 camera (Nikon, Abingdon, VA, USA). Sections were stained with hematoxylin and eosin (H&E), and analyzed by masked observers. Measurements (×400) were obtained at 1 mm dorsal and ventral from the optic disk.

Immunohistochemical studies

Antigen retrieval was performed by heating (90 °C) slices for 30 minutes in citrate buffer (pH 6.3) and then preincubated with 2% normal horse serum, 0.1% bovine serum albumin, and 0.4% Triton X-100 in 0.01 M PBS for 1 h. For immunodetection of glial cells, sections were incubated overnight at 4 °C with a mouse monoclonal anti- glial fibrillary acidic protein (GFAP) antibody conjugated to Cy3 (1:1200; Sigma Chemical Co., St Louis, MO, USA). For vascular endothelial growth factor (VEGF) immunodetection, paraffin sections were treated with 0.3% H_2O_2 in PBS for 20 min (for blocking endogenous peroxidase activity) and incubated overnight at 4 °C with a rabbit polyclonal anti-VEGF antibody (1:800; Calbiochem, La Jolla, CA, USA). Immunohistochemical detection was performed using the LSAB2 System-HRP (Dako, California, USA), based on biotin–streptavidin–peroxidase, and visualized using 3,3'-diaminobenzidine as cromogen. An Olympus BX50

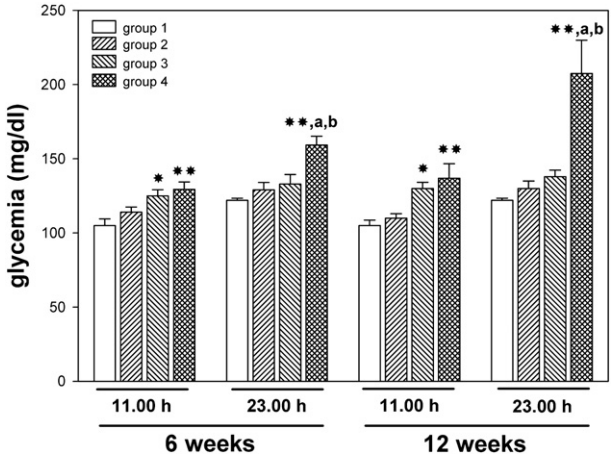

Fig. 4. Non-fasting glycemia assessed at 11.00 and 23.00 h. At 6 and 12 weeks of treatment, diurnal (i.e. at 11.00 h) plasma glucose levels were significantly higher in groups 3 and 4 as compared with group 1 (but not group 2), while nocturnal (i.e. at 23.00 h) glycemia in group 4 was significantly higher than in the other groups at both time points. Data are the mean ± SEM ($n = 10$ animals per group); $^{*}p<0.05$, $^{**}p<0.01$ vs. group 1, a: $p<0.01$ vs. group 2, b $p<0.01$ vs. group 3, by Tukey's test.

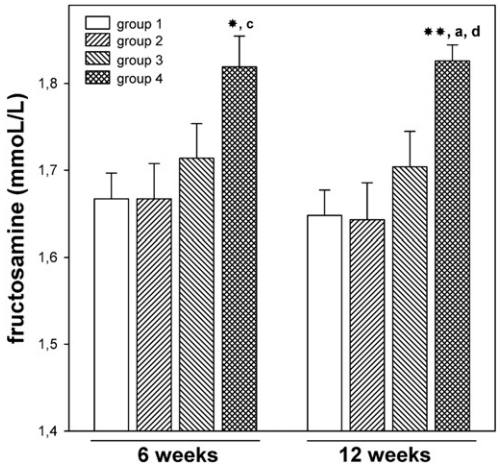

Fig. 5. Serum fructosamine levels at 6 and 12 weeks of treatment. Serum was extracted from 4 h fasted animals. At 6 weeks, fructosamine levels in group 4 significantly differed from groups 1 and 2, while at 12 weeks of treatment, this parameter was significantly higher in group 4 than in the other groups. Data are means ± SEM ($n = 10$ animals/group), $^{*}p<0.05$, $^{**}p<0.01$ vs. group 1 (control), a: $p<0.01$ vs. group 2, c: $p<0.05$ vs. group 2, d: $p<0.05$ vs. group 3, by Tukey's test.

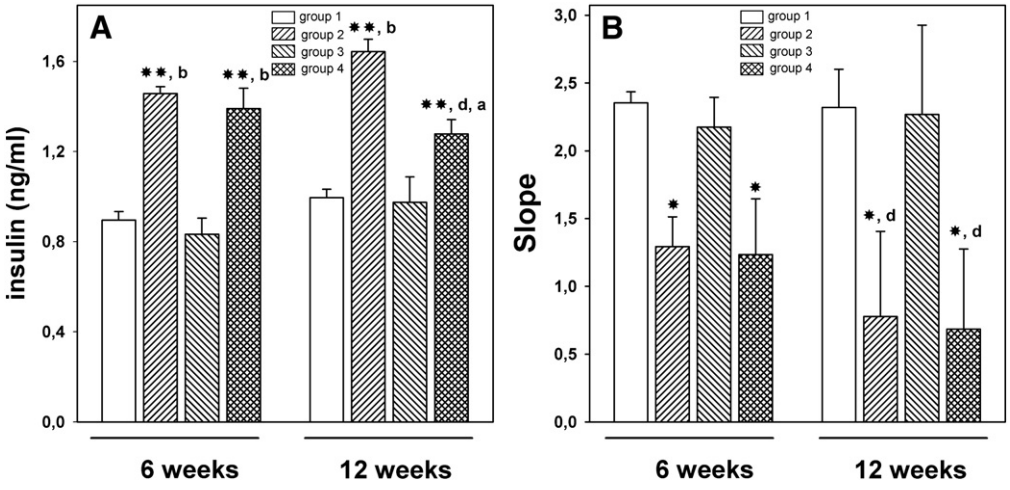

Fig. 6. Plasma insulin levels and IPITT at 6 and 12 weeks of treatment. Panel A: at both time points, plasmatic levels of insulin were significantly higher in groups 2 and 4 than in groups 1 and 3, but at 12 weeks of treatment, insulin levels were significantly lower in group 4 than in group 2. Panel B: rats were fasted for 4 h and then intraperitoneally injected with insulin (0.75 U/kg of body mass). Blood glucose levels were assessed before and 15, 30, 45 and 60 minutes after insulin administration. Insulin sensitivity was measured by the glucose disappearance rate within 60 min, evident from the average slope in the fitting curve. Higher insulin resistance was observed in groups 2 and 4 than in group 1 and 3. Data are means ± SEM ($n = 10$ animals/group), $^{*}p<0.05$, $^{**}p<0.01$ vs. group 1 (control), a: $p<0.01$ vs. group 2, b: $p<0.01$ vs. group 3, d: $p<0.05$ vs. group 3, by Tukey's test.

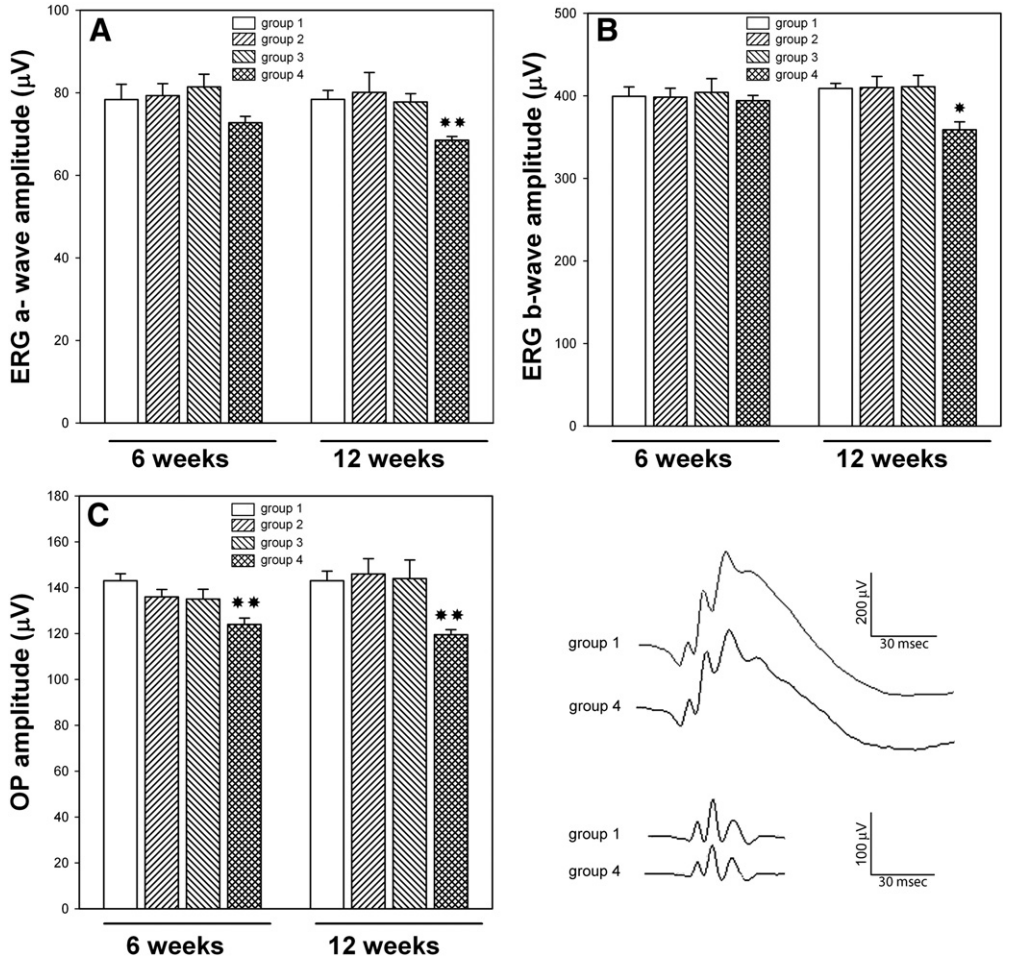

Fig. 7. Scotopic ERGs at 6 and 12 weeks of treatment. Average amplitudes of scotopic ERG a- wave (panel A) and b-wave (panel B). At 12 (but not 6) weeks of treatment, a significant decrease in the amplitude (but not their latencies) of both ERG a- and b-wave amplitude was observed in group 4 as compared with the other groups. Panel C: sum of OP amplitude. This parameter was significantly lower in group 4 than in the other groups at both time points. Panel D: representative scotopic ERG traces from groups 4 and 1 at 12 weeks of treatment. Data are the mean ± SEM ($n = 15$ animals per group), $^{*}p<0.05$, $^{**}p<0.01$ vs. groups 1, 2, and 3, by Tukey's test.

microscope (Olympus, Tokyo, Japan) was used for microscopic observations.

NOS activity

Retinal NOS activity was assessed as previously described (Belforte et al., 2007). Each retina was homogenized in buffer solution containing 0.25 M sucrose and 20 mM HEPES (adjusted to pH 7.4 with Tris base). Reaction mixtures contained 50 μl of the enzyme source and 50 μl of a buffer stock solution containing 20 mM HEPES, 6 mM $CaCl_2$, 2.1 mM NADPH, 12.5 μM FAD, 2 mM β-mercaptoethanol, L-^{3}H-arginine (6 μCi/ml), and 2 μM L-arginine. After incubation at 37 °C for 30 min, the reaction was stopped by adding 200 μl of stop buffer (50 mM HEPES, 10 mM EDTA, and 10 mM EGTA, pH 5.5) and cooling the tubes for 5 min. The solution was mixed with resin Dowex AG50W-X8 (Na^+ form) to remove L-arginine, and centrifuged at 10,000*g* for 5 min. L-^{3}H-citrulline in the supernatant was quantified by liquid scintillation counting. Nonenzymatic conversion of L-^{3}H-arginine to L-^{3}H-citrulline was tested by adding buffer instead of the enzyme source.

Measurement of TBARS levels

TBARS levels in retinal tissue were analyzed as previously described (Ohkawa et al., 1979). Retinas were homogenized in 15 mM potassium buffer and 60 mM KCl, pH 7.4. The homogenate (300 μl) was mixed with 75 μl 10% SDS and 1.4 ml of 0.8 g% thiobarbituric acid dissolved in 10% acetic acid (pH 3.5). The solution was heated to 100 °C for 60 min. After cooling, the flocculent precipitate was removed by centrifugation at 3200 ×*g* for 10 min. After addition of 1 ml water and 5 ml of n-butanol-pyridine mixture (15:1, vol/vol), the mixture was vigorously shaken and centrifuged at 2000 ×*g* for 15 min. The absorbance of the organic layer was measured at an emission wavelength of 553 nm by using an excitation wavelength of 515 nm with a Jasco FP 770 fluorescence spectrophotometer (Japan Spectroscopic Co. Ltd. Japan). The range of the standard curves of malondialdehyde bis-dimethyl acetal (MDA) was 10–2000 pmol. Results were expressed as nanomoles MDA per milligram of protein.

Assay for TNFα levels assessment

Two retinas were homogenized in 150 μl of phosphate saline buffer (PBS) pH 7.0 supplemented with 10% fetal bovine serum heat inactivated and a cocktail of protease inhibitors. Samples were cleared by centrifugation for 10 min at 13,000 rpm. TNFα levels were determined as previously described (De Laurentiis et al., 2010), using specific rat enzyme-linked immunosorbent assays (ELISA) using antibodies and standards obtained from BD Biosciences, Pharmingen, San Diego, CA, USA, according to the manufacturer's instructions. The reaction was stopped and absorbance was read immediately at 450 nm on a microplate reader (Model 3550, BIO-RAD Laboratories, California, USA). TNF-α levels were expressed as pg/ml.

Protein level assessment

Protein content was determined by the method of Lowry et al. (1951) using bovine serum albumin as the standard.

Statistical analysis

Data are shown as mean ± SEM. Results were tested for normality using the Kolmogorov–Smirnoff approach. Statistical analysis was then performed by a two-way ANOVA, followed by Tukey's *post hoc* test.

Results

Metabolic studies

Fig. 2 depicts the temporal course of the body weight from group 1 (control), group 2 (sucrose), group 3 (STZ), and group 4 (sucrose + STZ). This parameter significantly increased throughout the experiment in all groups, but from week 7 to 12, it was significantly higher in animals receiving sucrose (groups 2 and 4) than in those which did not (groups 1 and 3). Fasting plasma glucose levels were assessed at 6 and 12 weeks of treatment (Fig. 3A). At both time points, this parameter was significantly higher in the sucrose + SZT group than in the control and sucrose groups, while at 12 weeks of treatment, fasting glucose levels were significantly higher in animals injected with STZ than in control animals. Results of the intraperitoneal glucose tolerance test (IPGTT) are shown in Fig. 3. Glucose levels assessed before, and 30, 60, 90, and 120 min after an i.p. administration of 1 g/kg glucose, and the average AUC are shown in Figs. 3B and C, respectively. At 6 and 12 weeks of treatment, higher values of AUC were observed for the sucrose + STZ group as compared with the control, sucrose, and STZ groups, while group 3 (STZ) differed from the control group. At 6 and 12 weeks of treatment, plasma glucose levels were assessed at 11.00 and 23.00 h in non fasted animals (Fig. 4). At 6 weeks, diurnal (i.e. at 11.00 h) glycemia was slightly (but significantly) higher in the STZ and sucrose + STZ groups as compared with control animals (but not the sucrose group), while at both time points, nocturnal (i.e. at 23.00 h) glycemia was significantly higher in the sucrose + STZ group than in the other groups. Furthermore, at 6 weeks of treatment, serum protein glycosylation (assessed by fructosamine levels) was significantly higher in the sucrose + STZ group than in the control and sucrose groups, while at 12 weeks, fructosamine levels in the sucrose + STZ group differed from all the other groups (Fig. 5). At 6 and 12 weeks of treatment, plasmatic levels of insulin were significantly higher in the sucrose and sucrose + STZ groups than in the control and STZ groups (Fig. 6A), but at 12 weeks of treatment, insulin levels were significantly lower in the sucrose + STZ group than in the sucrose group. In addition, insulin resistance was higher in the sucrose and sucrose + STZ groups than in control animals (Fig. 6B) at 6 and 12 weeks of treatment.

Retinal studies

The functional state of the retinas was analyzed by scotopic electroretinography. The average amplitude of scotopic electroretinogram (ERG) a- and b- waves at 6 and 12 weeks of treatment are depicted in Fig. 7, and representative scotopic ERG traces are also shown in Fig. 7. At 12 (but not 6) weeks of treatment, these parameters were significantly reduced in the sucrose + STZ group compared to the other groups. No differences in the ERG a- and b- wave latencies were observed among groups (data not shown). At 6 and 12 weeks of treatment, the sum of oscillatory potential (OP) amplitudes significantly decreased in the sucrose + STZ group, as shown in Fig. 7.

Retinal sections were examined by light microscopy at 12 weeks of treatment. The integrity of the laminar structure of the retina was intact in all groups (Fig. 8, upper panel). Retinal immunoreactivity for GFAP is shown in the middle panel of Fig. 8. In retinas from the control, sucrose, and STZ groups, astrocytes localized in the nerve fiber layer and ganglion cell layer (GCL) were GFAP-immunopositive, whereas in retinas from the sucrose + STZ group, an increase in retinal GFAP levels in glial processes from the inner limiting membrane to the outer retina associated with activated Müller cells was observed. The immunohistochemical assessment of VEGF is shown in the lower panel of Fig. 8. At

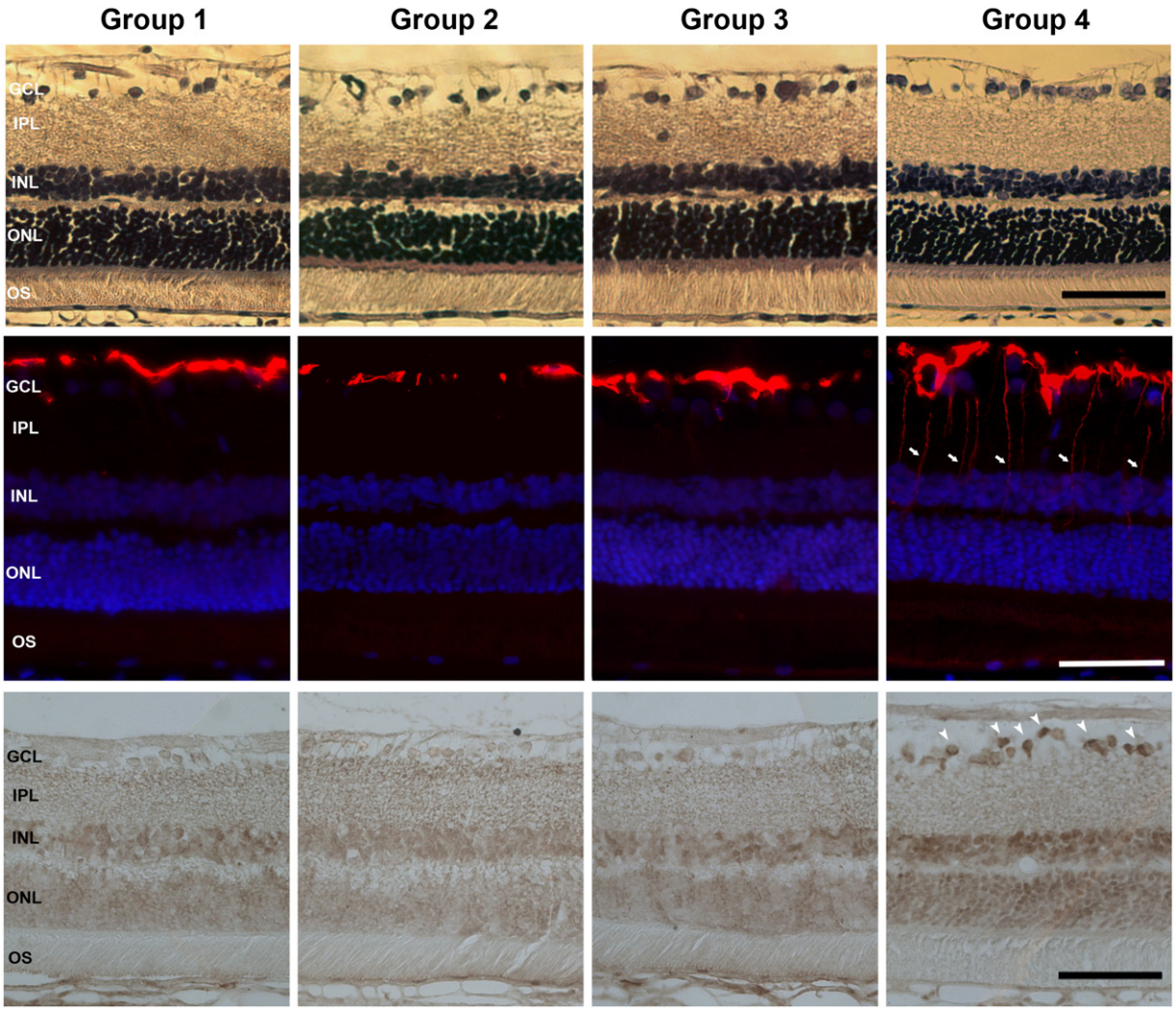

Fig. 8. Retinal histology study. Upper panel: representative photomicrographs of retinal sections from all the experimental groups stained with H&E. No evident changes in retinal morphology were observed among groups. Middle panel: Immunohistochemical detection of GFAP. In retinas from group 4, an intense GFAP (+) immunoreactivity was observed in astrocytes and glial processes from the inner limiting membrane to the outer retina associated with activated Müller cells (arrows), whereas in the other groups, GFAP immunostaining was restricted to astrocytes localized in the nerve fiber layer and GCL layer. Lower panel: VEGF in retinal sections. In retinas from groups 1, 2, and 3, a weak VEGF-immunoreactivity was diffusely observed throughout the inner retina. In retinas from group 4, intense immunoreactive perikarya in GCL cells (arrow head) and in some cells in the INL and ONL were observed. Scale bar: upper and lower panel = 100 μm; Middle panel = 50 μm. GCL, ganglion cell layer; IPL, inner plexiform layer; INL, inner nuclear layer; ONL, outer nuclear layer; OS, outer segments of photoreceptors.

12 weeks of treatment, VEGF levels in retinas from animals receiving sucrose + STZ (group 4) increased in comparison with retinas from the control, sucrose, and STZ groups. VEGF-immunolabeling was observed in perikarya of neurons in the GCL and some cells in the inner and outer nuclear layer.

Retinal NOS activity, TBARS (an index of lipid peroxidation), and TNFα levels were assessed after 12 weeks of treatment. These parameters were significantly higher in the sucrose + STZ group than in the other groups (Fig. 9). In addition, retinal lipid peroxidation in the sucrose group was significantly higher than in group 1. At 6 weeks of treatment, VEGF, GFAP, TBARS and TNFα levels and NOS activity did not differ among groups (data not shown).

Discussion

The present results indicate that the combination of diet-induced insulin resistance and a slight secretory impairment resulting from a low-dose STZ treatment mimicked some features of the diabetic state observed in patients with mild T2DM at its initial stages: slight fasting hyperglycemia, hyperinsulinemia, and elevated postprandial (nocturnal) glycemic levels. Noteworthy, only animals exposed to this combined treatment developed significant retinal alterations, whereas each one of these maneuvers *per se* (a sucrose-enriched diet or a STZ injection) did not induce significant retinal changes. The main metabolic characteristic which differentiated the combined treatment from the other groups was a comparatively high glucose level in the non-fasting state.

The metabolic profile resulting from this combined treatment contrasts sharply with that arising from the widely used STZ-induced type 1 diabetes rat model. High doses of STZ rapidly lead to destruction of pancreatic β-cells with acute insulin deficiency, body weight loss, and a pronounced reduction of lifespan, which markedly differ from the clinical and metabolic features that characterize human T2DM. In contrast, the dose of STZ used in this work was a sub-threshold dose, as shown by the fact that it did not affect *per se* fasting plasma insulin levels.

The early stages of T2DM, arising as a consequence of enhanced insulin resistance and a mild, but significant impairment in insulin secretion, and showing mild, or even absent, fasting hyperglycemia and marked postprandial hyperglycemia, were accurately reproduced in our model.

Rodents are nocturnal feeders with approximately 70% of their daily caloric intake occurring during the dark phase (Ayala et al., 2006). Therefore, we assessed plasma glucose levels at 11.00 h and 23.00 h, corresponding to periods of fasting and feeding respectively. At 23.00 h, markedly elevated glycemic levels (~200 mg/dl) were detected in rats submitted to the combined treatment, in contrast to those measured in the other groups. Nocturnal non-fasting hyperglycemia is likely to account for the increase in fructosamine levels in this group.

In diabetic patients, abnormal visual function usually precedes morphological alterations that characterize DR (Bresnick and Palta, 1987; Gardner et al., 2002; Juen and Kieselbach, 1990). The function of the neural components of the middle and inner retinal layers, as assessed by the ERG, is altered in persons with diabetes prior to the development of fundoscopically evident retinopathic changes. Thus, the ERG is considered a sensitive marker of early neuronal abnormalities, long before DR can be clinically detected (Tzekov and Arden, 1999). The most common ERG abnormality in diabetic patients without clinically evident retinopathy is a reduction in the amplitude and/or an increase in OP implicit time (Holopigian et al., 1992; Juen and Kieselbach, 1990; Wachtmeister, 1998). Other ERG abnormalities in persons with diabetes without retinopathy include a reduction in the scotopic b-wave amplitude (Holopigian et al., 1992; Juen and Kieselbach, 1990). In agreement, a significant decrease in OP amplitude was observed in animals submitted to the combined treatment for 6 and 12 weeks, while slight (but significant) alterations in the scotopic ERG were observed in animals submitted to the combined treatment for 12 weeks, without major changes in retinal morphology. Present results further support that OPs could be an early indicator of retinal alterations in a diabetic-like background. Whether retinal alterations in the sucrose-fed/STZ model further progress over longer periods is unknown at this time, and will be examined in the near future.

It has been postulated that Müller cells may be critical in the initial steps of retinopathy in T2DM. Müller cells that do not express GFAP under physiological conditions are known to express GFAP in pathological situations (Erickson et al., 1987; Osborne et al., 1991). As shown herein, the combined treatment provoked a significant increase in Müller cell GFAP immunoreactivity. In agreement, it was shown that GFAP is upregulated in Müller cells in the type 1 diabetes rat model induced by STZ (Hammes et al., 1995).

Although the pathogenesis of DR is still far from being fully understood, VEGF is recognized as a major contributor to its development, and is implicated as the initiator and mediator of non-proliferative and proliferative DR (Aiello and Wong, 2000; Lutty et al., 1996). In fact, clinical trials using anti-VEGF therapies are showing promising results against advanced stages of DR (Arevalo et al., 2007; Ng and Adamis, 2006). Our results indicate that only the combined treatment induced a significant increase in retinal VEGF levels.

Several studies reported that oxidative and nitrosative stress are increased in diabetic patients and play an important role in

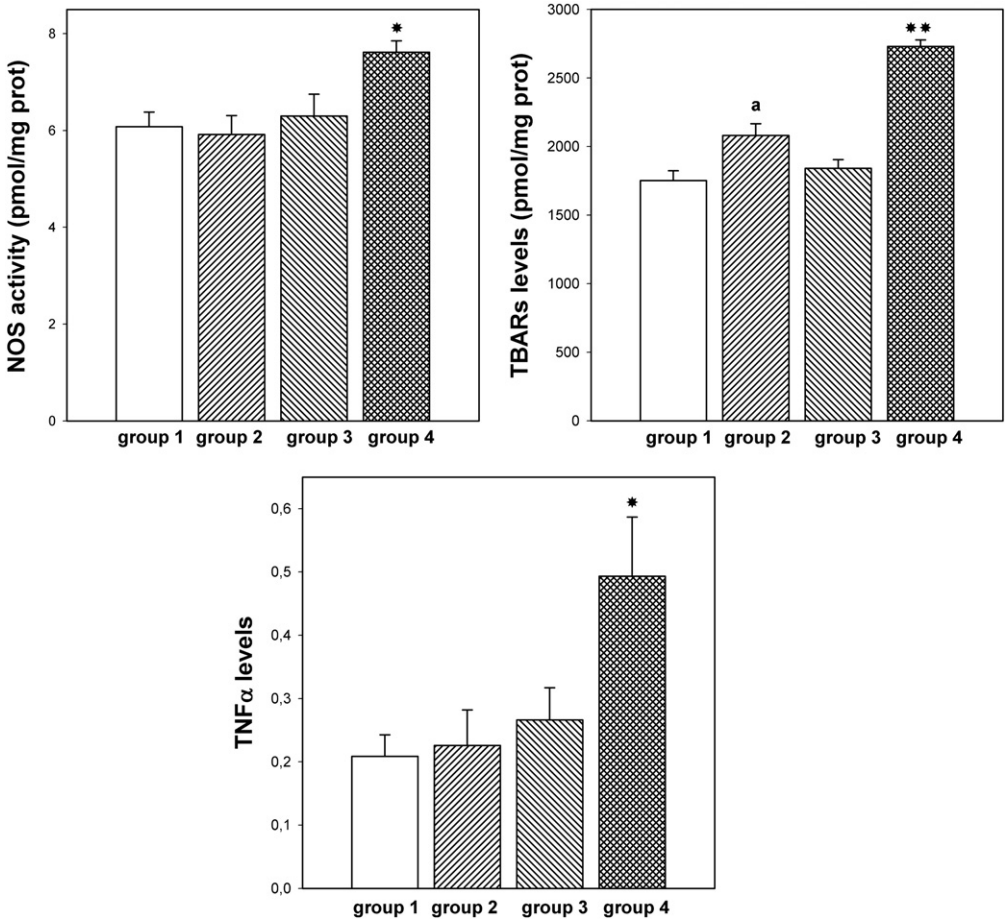

Fig. 9. Retinal NOS activity, TBARS, and TNFα levels assessed at 12 weeks of treatment. These parameters were significantly higher in group 4 than in groups 1, 2, and 3, while TBARS levels were higher in group 2 than in group 1. Data are mean ± SE ($n = 10$ retinas/group), $^{*}p<0.05$, $^{**}p<0.01$ vs. groups 1, 2, and 3, a: $p<0.05$ vs. group 1, by Tukey's test.

the pathogenesis of diabetic complications, including retinopathy (Mokini et al., 2010; Zheng and Kern, 2009). A significant increase in retinal lipid peroxidation and NOS activity was observed in animals subjected to the combined treatment. In agreement, a significant increase in retinal NOS activity was previously described in four months Goto–Kakizaki rats, a non-insulin-dependent model of diabetes (Carmo et al., 2000). In DR, abnormalities in vascular and neuronal function are closely related to the local production of inflammatory mediators (Kaul et al., 2010). In this regard, a significant increase in retinal TNFα levels was observed in rats submitted to the combined treatment. Taken together, these results suggest that the combined treatment exhibited characteristics of the early phase of DR. These findings do not imply that this model is superior to other rat models of T2DM. However, there are important differences worth of commenting. For example, rats submitted to a high fructose diet which develop several symptoms of T2DM (such as insulin resistance and glucose intolerance) do not show signs of retinopathy even after 16 weeks of treatment (Patel et al., 2009). In spontaneously diabetic Torii (SDT) fatty rats (a model of obese T2DM) significant alterations in the ERG were evident at 16 weeks of age, whereas in SDT normal rats (a model of non-obese T2DM), 32 weeks of age were needed to induce a retinal dysfunction (Matsui et al., 2008). In sucrose-fed *Wistar* rats injected with a moderate dose of STZ, retinal alterations occurred earlier than those observed in other experimental models (adulthood onset). The early onset of diabetes-associated ERG alterations could be an advantage for the use of this model in diabetes research, mainly considering that changes in the ERG can be influenced by aging (Li et al., 2001; Weleber, 1981). Moreover, these results suggest that normal or near-normal fasting plasma glucose levels and marked postprandial glycemic excursions induced retinal alterations, which are compatible with early stages of human T2DM.

Conclusions

The present results indicate that the combination of diet-induced insulin resistance and a slight secretory impairment induced by a low-dose of STZ, which was neither inbred nor genetically obese, easily available, and relatively inexpensive, reproduced some metabolic characteristics of human T2DM, and promoted early signs of DR. Thus, this model could offer the opportunity to investigate DR at an early stage in a setting of moderately altered glucose metabolism, which shows increasing prevalence worldwide.

Disclosures

This research was supported by grants from the Agencia Nacional de Promoción Científica y Tecnológica (ANPCyT), The University of Buenos Aires, and CONICET, Argentina. Authors declare no financial or other relationships that might lead to a conflict of interest.

Acknowledgments

The authors thank Enzo Aran Cuba for its invaluable help in animal care.

References

Aiello, L.P., Wong, J.S., 2000. Role of vascular endothelial growth factor in diabetic vascular complications. Kidney Int. 77, S113–S119.
American Diabetes Association, 2008. Diagnosis and classification of diabetes mellitus. Diabetes Care 31, S55–S60.
Arevalo, J.F., Fromow-Guerra, J., Quiroz-Mercado, H., Sanchez, J.G., Maia, M., Berrocal, M.H., Solis-Vivanco, A., Farah, M.E., Pan-American Collaborative Retina Study Group, 2007. Primary intravitreal bevacizumab (Avastin) for diabetic macular edema: results from the Pan-American Collaborative Retina Study Group at 6-month follow-up. Ophthalmology 114, 743–750.
Ayala, J.E., Bracy, D.P., McGuinness, O.P., Wasserman, D.H., 2006. Considerations in the design of hyperinsulinemic–euglycemic clamps in the conscious mouse. Diabetes 55, 390–397.
Belforte, N., Moreno, M.C., Cymeryng, C., Bordone, M., Keller Sarmiento, M.I., Rosenstein, R.E., 2007. Effect of ocular hypertension on retinal nitridergic pathway activity. Invest. Ophthalmol. Vis. Sci. 48, 2127–2133.
Bray, G.A., 2004. Medical consequences of obesity. J. Clin. Endocrinol. Metab. 89, 2583–2589.
Bresnick, G.H., Palta, M., 1987. Temporal aspects of the electroretinogram in diabetic retinopathy. Arch. Ophthalmol. 105, 660–664.
Carmo, A., Cunha-Vaz, J.G., Carvalho, A.P., Lopes, M.C., 2000. Nitric oxide synthase activity in retinas from non-insulin-dependent diabetic Goto–Kakizaki rats: correlation with blood-retinal barrier permeability. Nitric Oxide 4, 590–596.
Danaei, G., Finucane, M.M., Lu, Y., Singh, G.M., Cowan, M.J., Paciorek, C.J., Lin, J.K., Farzadfar, F., Khang, Y.H., Stevens, G.A., Rao, M., Ali, M.K., Riley, L.M., Robinson, C.A., Ezzati, M., Global burden of metabolic risk factors of chronic diseases collaborating group (blood glucose), 2011. National, regional, and global trends in fasting plasma glucose and diabetes prevalence since 1980: systematic analysis of health examination surveys and epidemiological studies with 370 country-years and 2·7 million participants. Lancet 378, 31–40.
De Laurentiis, A., Fernandez-Solari, J., Mohn, C., Burdet, B., Zorrilla Zubilete, M.A., Rettori, V., 2010. The hypothalamic endocannabinoid system participates in the secretion of oxytocin and tumor necrosis factor-alpha induced by lipopolysaccharide. J. Neuroimmunol. 221, 32–41.
Diabetes Control and Complications Trial Research Group, 1993. Hypoglycemia in the diabetes control and complications trial. Diabetes 46, 271–286.
Erickson, P.A., Fisher, S.K., Guerin, C.J., Anderson, D.H., Kaska, D.D., 1987. Glial fibrillary acidic protein increases in Müller cells after retinal detachment. Exp. Eye Res. 44, 37–48.
Gardner, T.W., Antonetti, D.A., Barber, A.J., LaNoue, K.F., Levison, S.W., 2002. Diabetic retinopathy: more than meets the eye. Surv. Ophthalmol. 47, 253–262.
Goralski, K.B., Sinal, C.J., 2007. Type 2 diabetes and cardiovascular disease: getting to the fat of the matter. Can. J. Physiol. Pharmacol. 85, 113–132.
Hammes, H.P., Federoff, H.J., Brownlee, M., 1995. Nerve growth factor prevents both neuroretinal programmed cell death and capillary pathology in experimental diabetes. Mol. Med. 1, 527–534.
Holopigian, K., Seiple, W., Lorenzo, M., Carr, R., 1992. A comparison of photopic and scotopic electroretinographic changes in early diabetic retinopathy. Invest. Ophthalmol. Vis. Sci. 33, 2773–2780.
Juen, S., Kieselbach, G.F., 1990. Electrophysiological changes in juvenile diabetics without retinopathy. Arch. Ophthalmol. 108, 372–375.
Kaul, K., Hodgkinson, A., Tarr, J.M., Kohner, E.M., Chibber, R., 2010. Is inflammation a common retinal–renal–nerve pathogenic link in diabetes? Curr. Diabetes Rev. 6, 294–303.
King, H., Aubert, R.E., Herman, W.H., 1998. Global burden of diabetes, 1995–2025: prevalence, numerical estimates, and projections. Diabetes Care 21, 1414–1431.
Li, C., Cheng, M., Yang, H., Peachey, N.S., Naash, M.I., 2001. Age-related changes in the mouse outer retina. Optom. Vis. Sci. 78, 425–430.
Lowry, O.H., Rosebrough, N.J., Farr, A.L., Randall, R.J., 1951. Protein measurement with the Folin phenol reagent. J. Biol. Chem. 193, 265–275.
Lutty, G.A., McLeod, D.S., Merges, C., Diggs, A., Plouét, J., 1996. Localization of vascular endothelial growth factor in human retina and choroid. Arch. Ophthalmol. 114, 971–977.
Matsui, K., Ohta, T., Oda, T., Sasase, T., Ueda, N., Miyajima, K., Masuyama, T., Shinohara, M., Matsushita, M., 2008. Diabetes-associated complications in Spontaneously Diabetic Torii fatty rats. Exp. Anim. 57, 111–121.
Matsumura, T., Yamagishi, S., Kodama, Y., Shibata, R., Ueda, S., Narama, I., 2005. Otsuka Long–Evan Tokushima Fatty (OLETF) rat is not a suitable animal model for the study of angiopathic diabetic retinopathy. Int. J. Tissue React. 27, 59–62.
Mokini, Z., Marcovecchio, M.L., Chiarelli, F., 2010. Molecular pathology of oxidative stress in diabetic angiopathy: role of mitochondrial and cellular pathways. Diabetes Res. Clin. Pract. 87, 313–321.
Monnier, L., Colette, C., Dunseath, G.J., Owens, D.R., 2007. The loss of postprandial glycemic control precedes stepwise deterioration of fasting with worsening diabetes. Diabetes Care 30, 263–269.
Moreno, M.C., Marcos, H.J., Oscar Croxatto, J., Sande, P.H., Campanelli, J., Jaliffa, C.O., Benozzi, J., Rosenstein, R.E., 2005. A new experimental model of glaucoma in rats through intracameral injections of hyaluronic acid. Exp. Eye Res. 81, 71–80.
Movassat, J., Saulnier, C., Portha, B., 1995. Beta-cell mass depletion precedes the onset of hyperglycemia in the GK rat, a genetic model of non-insulin dependent diabetes mellitus. Diabetes Metab. 21, 365–370.
Mühlhausler, B.S., 2009. Nutritional models of type 2 diabetes mellitus. Methods Mol. Biol. 560, 19–36.
Ng, E.W., Adamis, A.P., 2006. Anti-VEGF aptamer (pegaptanib) therapy for ocular vascular diseases. Ann. N. Y. Acad. Sci. 1082, 151–171.
Ohkawa, H., Ohishi, N., Yagi, K., 1979. Assay for lipid peroxides in animal tissues by thiobarbituric acid reaction. Anal. Biochem. 95, 351–358.
Osborne, N.N., Block, F., Sontag, K.H., 1991. Reduction in ocular blood flow results in glial fibrillary acidic protein (GFAP) expression in rat Müller cells. Vis. Neurosci. 7, 637–639.
Patel, J., Iyer, A., Brown, L., 2009. Evaluation of the chronic complications of diabetes in a high fructose diet in rats. Indian J. Biochem. Biophys. 46, 66–72.

Portha, B., Blondel, O., Serradas, P., McEvoy, R., Giroix, M.H., Kergoat, M., Bailbe, D., 1989. The rat models of non-insulin dependent diabetes induced by neonatal streptozotocin. Diabetes Metab. 15, 61–75.

Shafrir, E., Ziv, E., Kalman, R., 2006. Nutritionally induced diabetes in desert rodents as models of type 2 diabetes: *Acomys cahirinus* (spiny mice) and *Psammomys obesus* (desert gerbil). ILAR J. 47, 212–224.

Srinivasan, K., Ramarao, P., 2007. Animal models in type 2 diabetes research: an overview. Indian J. Med. Res. 125, 451–472.

Srinivasan, K., Viswanad, B., Asrat, L., Kaul, C.L., Ramarao, P., 2005. Combination of high-fat diet-fed and low-dose streptozotocin-treated rat: a model for type 2 diabetes and pharmacological screening. Pharmacol. Res. 52, 313–320.

Surwit, R.S., Kuhn, C.M., Cochrane, C., McCubbin, J.A., Feinglos, M.N., 1988. Diet-induced type II diabetes in C57BL/6J mice. Diabetes 37, 1163–1167.

The Eye Diseases Research Prevalence Research Group-National Eye Institute, 2004. The prevalence of diabetic retinopathy among adults in the United States. Arch. Ophthalmol. 122, 552–563.

Tzekov, R., Arden, G.B., 1999. The electroretinogram in diabetic retinopathy. Surv. Ophthalmol. 44, 53–60.

UK Prospective Diabetes Study (UKPDS) Group, 1998. Effect of intensive blood-glucose control with metformin on complications in overweight patients with type 2 diabetes (UKPDS 34). Lancet 352, 854–865.

Wachtmeister, L., 1998. Oscillatory potentials in the retina: what do they reveal. Prog. Retin. Eye Res. 17, 485–521.

Weleber, R.G., 1981. The effect of age on human cone and rod ganzfeld electroretinograms. Invest. Ophthalmol. Vis. Sci. 20, 392–399.

Zheng, L., Kern, T.S., 2009. Role of nitric oxide, superoxide, peroxynitrite and PARP in diabetic retinopathy. Front. Biosci. 14, 3974–3987.